Journal of Alloys and Compounds 483 (2009) 484–487

Contents lists available at ScienceDirect

Journal of Alloys and Compounds

journal homepage: www.elsevier.com/locate/jallcom

Kinetics of mechanochemical synthesis of Me/FeS (Me = Cu, Pb, Sb) nanoparticles

P. Baláž [a,*], E. Dutková [a], I. Škorvánek [b], E. Gock [c], J. Kovac [d], A. Satka [d]

[a] Institute of Geotechnics, Slovak Academy of Sciences, Watsonova 45, 043 53 Košice, Slovakia
[b] Institute of Experimental Physics, Slovak Academy of Sciences, Watsonova 47, 043 53 Košice, Slovakia
[c] Institute of Mineral and Waste Processing and Dumping Technology, Technical University Clausthal, Walther-Nernst Strasse 9, 38678 Clausthal-Zellerfeld, Germany
[d] Department of Microelectronics, Slovak University of Technology and International Laser Centre, 812 19 Bratislava, Slovakia

ARTICLE INFO

Article history:
Received 30 August 2007
Received in revised form 24 July 2008
Accepted 26 July 2008
Available online 18 December 2008

Keywords:
Metals
Nanostructures
High-energy ball milling
Mechanochemical synthesis
Solid-state kinetics

ABSTRACT

The mechanochemical synthesis of Cu/FeS, Pb/FeS and Sb/FeS nanoparticles was investigated with the regard to solid-state kinetics. Experiments were performed in a planetary mill and in an eccentric vibratory mill by a high-energy milling of Cu_2S, PbS and Sb_2S_3, respectively with elemental iron under protective atmosphere. Cu, Pb and Sb nanometals were obtained due to the reducing power of iron. The reduction processes are very straightforward and fast and can be carried out at ambient temperature. Nanometals are embedded into FeS matrix forming metal/ceramics nanocomposites. XRD, SEM and magnetometry methods were used to characterize the ball-milled products. Solid-state kinetics has been evaluated based on magnetometry data.

1. Introduction

Recently, mechanochemical processing via high-energy milling has been reviewed as means of the synthesis of a wide variety of nanocrystalline materials [1–3]. The chemical reactions occur at the interfaces of the nanometer size grains that are continually regenerated during milling. As a consequence, reactions that would normally require high temperatures to occur due to the separation of the reacting phases by the products phases, can proceed at low temperature in a ball mill.

Mechanochemical solid-state reduction of sulphides to prepare nanocrystalline products can be schematically expressed by general equation

$$Me_1S + Me_2 \rightarrow Me_1 + Me_2S \quad (1)$$

where Me_1 is reduced metal and Me_2 is reducing metal. Several papers have been published using iron metal as reducing element [4–10]. The reactions are thermodynamically feasible at ambient temperature, as the enthalpy change ΔH°_{298} is negative (Table 1).

Various nanostructures have been identified in products of reactions (2)–(6) by XRD, Mössbauer, SEM and TEM methods.

The aim of this paper is to illustrate the progress in the mechanochemical preparation of nanometals from corresponding sulphides by applying solid-state kinetics approach based on processing of magnetometry data.

2. Experimental

2.1. Synthesis

Mechanochemical reduction of metal sulphides Cu_2S, PbS and Sb_2S_3 with elemental iron as reducing element in a ratio corresponding to Eqs. (2)–(4) was performed in a Pulverisette 6 laboratory planetary mill (Fritsch, Germany). A 250-ml tungsten carbide (WC) grinding chamber and 50 WC balls of 10 mm diameter (total weight 360 g) were used. The weight of the milled powder charge was 3 g. The speed of the planet carrier was set to 500 rpm. Milling times between 1 and 180 min were applied. The atmosphere inside the milling chamber was argon. The same reactions were also performed in an industrial eccentric vibratory mill ESM 654 (Siebtechnik, Germany). Milling was carried out in air for durations between 30 and 120 min. The milling chamber was filled with tungsten carbide balls and the weight of milled powder mixture was 100 g. The speed of the mill eccenter was 960 rpm.

2.2. Characterization

X-ray diffraction measurements were carried out using a Philips X'Pert diffractometer (the Netherlands), working in Θ–Θ geometry with CuK_α radiation. The XRD lines were identified by comparing the measured patterns to the JCPDS data cards. The morphology of samples was analyzed using FE-SEM LEO 1550 scanning microscope (Germany). The samples were not covered with any conductive material in order to avoid artefacts. Magnetization data were obtained by employing a vibrating sample magnetometer (VSM) equipped with a superconducting coil. The magnetic field was increased up to 3 T in order to assure the magnetic saturation of the specimens at room temperature.

---

[*] Corresponding author. Tel.: +421 55 7922603; fax: +421 55 7922604.
E-mail address: balaz@saske.sk (P. Baláž).

0925-8388/$ – see front matter © 2008 Elsevier B.V. All rights reserved.
doi:10.1016/j.jallcom.2008.07.151

Table 1
Mechanochemically induced solid-state reactions of metal sulphides with iron.

Reaction	ΔH°_{298} (kJ mol^{-1})
$Cu_2S + Fe \rightarrow 2Cu + FeS$ (2)	−21.0
$PbS + Fe \rightarrow Pb + FeS$ (3)	−1.3
$Sb_2S_3 + 3Fe \rightarrow 2Sb + 3FeS$(4)	−116.7
$FeS_2 + Fe \rightarrow 2FeS$ (5)	−13.3
$As_2S_3 + 3Fe \rightarrow 2As + 3FeS$(6)	−160.7

2.3. Kinetics processing

Avrami–Erofeev equation [11,12] in the form

$$-\ln(1-x) = kt^n \tag{7}$$

has been applied for processing of kinetic data. In Eq. (7) n is the order of reaction and k is the reaction rate constant. The conversion parameter x can be taken from the magnetometry data. Mathematical transformation of Eq. (7) leads to Eq. (8)

$$\ln(-\ln(1-x)) = n \ln k + n \ln t \tag{8}$$

allowed to calculate the order of the reaction n from the slope of the $\ln(-\ln(1-x))$ as a function of $\ln t$.

3. Results and discussion

3.1. Mechanochemical synthesis and product characterization

The progress of the nanocopper (grain size 20–30 nm) formation from copper sulphide (see Eq. (2) in Table 1) is illustrated by XRD patterns in Fig. 1A. The primary process – the reduction of Cu_2S by Fe while Cu metal and FeS are formed – is clearly seen, particularly by inspecting the relative intensities of the diffraction lines of Cu and Fe metal. With increase time of milling cubic FeS changes to its hexagonal modification troilite FeS [5]. This phase is considered to be the stable modification of stoichiometric iron sulphide.

The reaction between galena PbS and elemental Fe has been applied to obtain nanocrystalline lead (grain size 13–21 nm) according to Eq. (3) in Table 1 [6]. The XRD patterns are given in Fig. 1B. The process of mechanochemical reduction of PbS is evident. The significant line broadening suggests dramatical grain size reduction. After 60 min of milling, the reflection of well crystallized lead metal and cubic FeS can be observed with a relative high conversion.

The preparation of the nanoantimony by milling antimony sulphide with elemental iron as described by Eq. (3) in Table 1 has been performed in an industrial mill. XRD patterns are given in Fig. 1C. The most reduction is complete after 60 min of milling in a planetary mill. The grain size of antimony was found to be 19 nm with 0.35% residual strain [9,10].

Fig. 2A–C shows the room temperature magnetization data for investigated samples as a function of external magnetic field. It is evident that the resulting magnetization curves are well saturated after an application of higher magnetic fields. The difference in the saturation magnetization of the samples milled for different times is mainly caused by a various amount of the ferromagnetic component in these samples which is bcc-Fe.

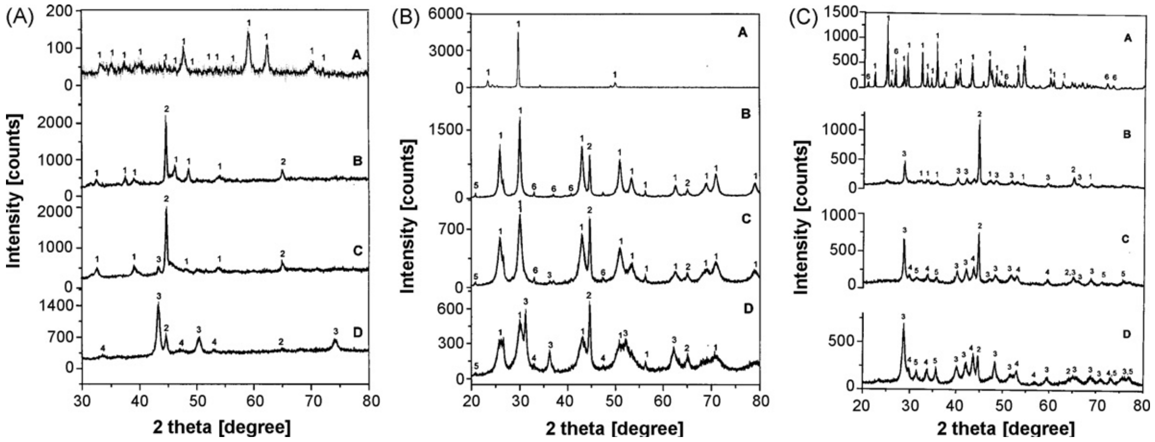

Fig. 1. (A) XRD patterns in the copper/iron sulphide system. A: starting Cu_2S. The milling times for patterns B–D are 30, 60 and 120 min, respectively (1: copper sulphide, 2: iron, 3: copper, 4: pyrrhotite, 5: quartz). (B) XRD patterns in the lead/iron sulphide system. A: starting PbS. The milling times for patterns B–D are 30, 60 and 120 min, respectively (1: lead sulphide, 2: iron, 3: lead, 4: pyrrhotite, 5: quartz, 6: pyrite). (C) XRD patterns in the antimony/iron sulphide system. A: starting Sb_2S_3. The milling times for patterns B–D are 30, 60 and 120 min, respectively (1: antimony sulphide, 2: iron, 3: antimony, 4: pyrrhotite, 5: tungsten carbide, 6: quartz).

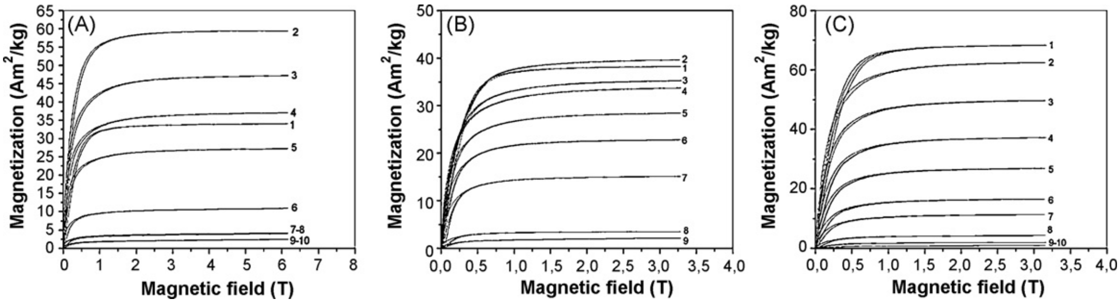

Fig. 2. (A) Magnetization as a function of external magnetic field in the copper/iron sulphide system. The milling times for patterns (1–6) are: 1: 0 min, 2: 1 min, 3: 4 min, 4: 6 min, 5: 10 min, 6: 20 min, 7: 25 min, 8: 30 min, 9: 35 min, 10: 40 min. (B) Magnetization as a function of external magnetic field in the lead/iron sulphide system. The milling times for patterns (1–9) are: 1: 0 min, 2: 10 min, 3: 20 min, 4: 30 min, 5: 40 min, 6: 50 min, 7: 90 min, 8: 120 min, 9: 180 min. (C) Magnetization as a function of external magnetic field in the antimony/iron sulphide system. The milling times for patterns (1–10) are: 1: 0 min, 2: 10 min, 3: 20 min, 4: 30 min, 5: 40 min, 6: 50 min, 7: 60 min, 8: 90 min, 9: 120 min, 10: 180 min.

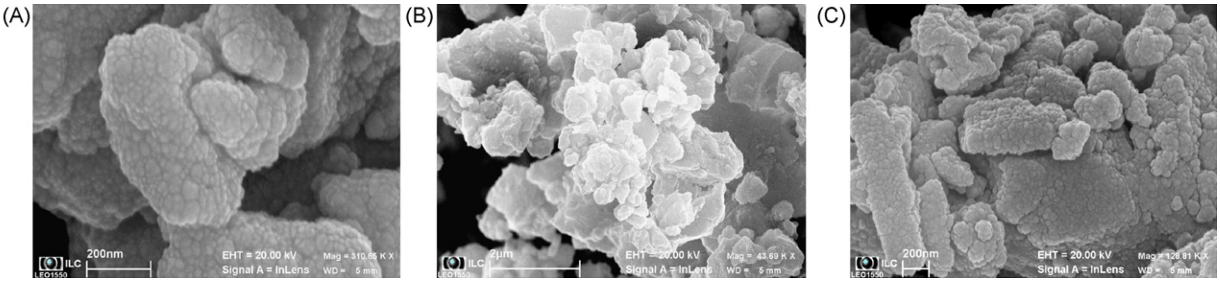

Fig. 3. SEM images in Me/FeS systems: (A) Cu/FeS, (B) Pb/FeS, (C) Sb/FeS.

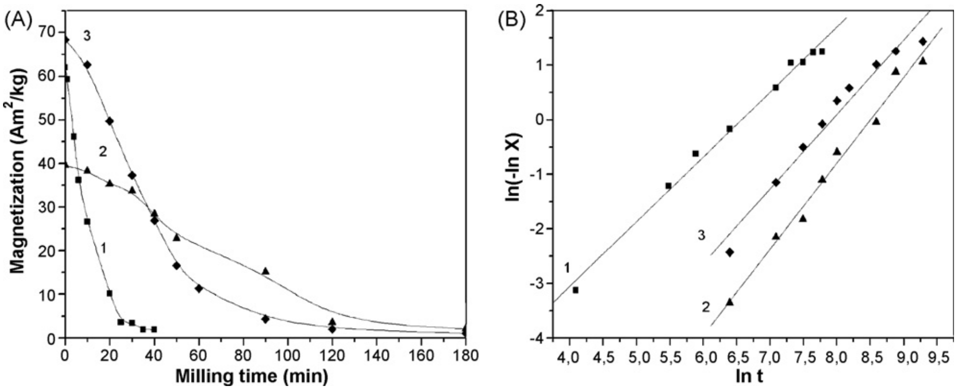

Fig. 4. (A) Kinetics of the mechanochemical synthesis of Me/FeS nanoparticles, Me = 1 – Cu, 2 – Pb, 3 – Sb. (B) $\ln(-\ln x)$ vs. $\ln t$ plots showing the application of Avrami–Erofeev equation.

Table 2
Calculated parameters of Avrami–Erofeev Eq. (7) for mechanochemically induced solid-state reactions of metal sulphides with iron.

Reaction	Parameter	
	k (s^{-1})	n
$Cu_2S + Fe \rightarrow 2Cu + FeS$ (2)	0.0014	1.1885
$PbS + Fe \rightarrow Pb + FeS$ (3)	0.0002	1.5787
$Sb_2S_3 + 3Fe \rightarrow 2Sb + 3FeS$(4)	0.0004	1.3650

SEM images of synthesized nanocomposites are seen in Fig. 3A–C. According to the observed surface morphology individual nanoparticles have tendency to form nanoparticle agglomerates during milling process. The solid-state recombination of nanoparticles into agglomerates is a general phenomenon which reflects a tendency of nanoparticulate systems to compensate unsaturated surface forces via surface reconstruction.

3.2. Solid-state kinetics

The kinetics of the solid-state reactions (2), (3) and (4) in Table 1 has been studied assuming the nucleation and crystal growth take place at nanostructures formation. The Avrami–Erofeev Eq. (7) has been applied for the kinetics description. The same procedure has been applied in paper [13] for single-step displacement reduction of hematite with magnesium.

The kinetic data for calculation of parameters k and n of Eq. (7) have been obtained from the magnetometry data presented for all three systems under study in Fig. 4. The calculated parameters are given in Table 2.

The rate of the nanometals preparation is in the order Cu > Sb > Pb. Kinetic Eq. (7) has been derived on assumption of three-dimensional growth of nuclei and is well suited for description of our processes. The parameter k with some approximation has meaning of the overall rate constant [14]. The parameter n is function of nuclei number and their shape, composition of initial reactants and products as well as gives information about reaction mechanismus [15]. The value of this parameter enables to resolve kinetic ($n \geq 1$) and diffusion ($n \sim 0.5$) regimes of solid-state reactions [16]. According to this statement, our experimental data in Table 2 show that the kinetic regime is the rate-determining step for all the systems under study.

4. Conclusions

1. Nanocrystalline copper, lead and antimony metals were prepared by mechanochemical reduction of the corresponding metal sulphides.
2. Elemental iron has been proven as an effective reducing agent for sulphide reduction.
3. Magnetization data were utilized for a rate of solid-state kinetics calculation.

Acknowledgements

The support through the Slovak Research and Developing Agency (project APVV 0347-06, VVCE-0049-07), the Slovak Grant Agency VEGA (project 2/0035/08, 1/689/09), Center of Excellence of the Slovak Academy of Sciences (project NANOSMART), DAAD-PPT project and International Laser Center in Bratislava (SEM measurements) is gratefully acknowledged.

References

[1] L. Takacs, Prog. Mater. Sci. 47 (2002) 355–461.

[2] E. Gaffet, G. Le Caër, in: H.S. Nalwa (Ed.), Mechanical Processing for Nanomaterials, Encyclopedia of Nanoscience and Nanotechnology, vol. 5, American Scientific Publishers, New York, 2004, pp. 91–129.

[3] C. Suryanarayana, Mechanical Alloying and Milling, Marcel Dekker, New York, 2004.

[4] P. Matteazzi, G. Le Caër, Mater. Sci. Eng. A 156A (1992) 229–237.

[5] P. Baláž, L. Takacs, J.Z. Jiang, V. Soika, M. Luxová, Mater. Sci. Forum 386–388 (2002) 257–262.

[6] E. Godočíková, P. Baláž, E. Boldižárová, I. Škorvánek, J. Kováč, W.S. Choi, J. Mater. Sci. 39 (2004) 5353–5355.

[7] P. Baláž, A. Aláčová, E. Godočíková, J. Kováč, I. Škorvánek, J.Z. Jiang, Czech. J. Phys. 54 (2004) D197–D200.

[8] P. Baláž, E. Godočíková, L. Takacs, E. Gock, Int. J. Mater. Prod. Technol. 23 (2005) 26–41.

[9] P. Baláž, L. Takacs, E. Godočíková, I. Škorvánek, J. Kováč, W.S. Choi, J. Alloys Comp. 434–435 (2007) 773–775.

[10] E. Godočíková, P. Baláž, L. Takacs, V. Šepelák, I. Škorvánek, E. Gock, Metal. Mater. 45 (2007) 99–104.

[11] M. Avrami, J. Chem. Phys. 9 (1941) 177–184.

[12] B.V. Erofeev, Dokl. Akad. Nauk SSSR 52 (1946) 515–518.

[13] M. Sherif El-Eskandarany, H.N. El-Bahnasawy, H.A. Ahmed, N.A. Eissa, J. Alloys Comp. 314 (2001) 286–295.

[14] P. Barret, Kinetics of Heterogeneous Reactions in Solid-Gas Systems, Academia, Prague 1978 (in Czech).

[15] J.E. Christian, The Theory of Transformation in Metals and Alloys, Pergamon Press, New York, 1965.

[16] V.V. Boldyrev, Experimental Methods in Mechanochemistry of Solid Inorganic Materials, Nauka, Novosibirsk, 1983 (in Russian).